Chinese Journal of Electronics
Vol.32, No.2, Mar. 2023

Ergodic Capacity of NOMA-Based Overlay Cognitive Integrated Satellite-UAV-Terrestrial Networks

GUO Kefeng[1,2], LIU Rui[2], DONG Chao[1], AN Kang[3], HUANG Yuzhen[4], and ZHU Shibing[2]

(1. *College of Electronic and Information Engineering, Nanjing University of Aeronautics and Astronautics, Nanjing 210016, China*)

(2. *School of Space Information, Space Engineering University, Beijing 101416, China*)

(3. *The Sixty-third Research Institute, National University of Defense Technology, Nanjing 210007, China*)

(4. *Artificial Intelligence Research Center, National Innovation Institute of Defense Technology, Beijing 100166, China*)

Abstract — Satellite communication has become a popular study topic owing to its inherent advantages of high capacity, large coverage, and no terrain restrictions. Also, it can be combined with terrestrial communication to overcome the shortcomings of current wireless communication, such as limited coverage and high destructibility. In recent years, the integrated satellite-unmanned aerial vehicle-terrestrial networks (IS-UAV-TNs) have aroused tremendous interests to effectively reduce the transmission latency and enhance quality-of-service with improved spectrum efficiency. However, the rapidly growing access demands and conventional spectrum allocation scheme lead to the shortage of spectrum resources. To tackle the mentioned challenge, the non-orthogonal multiple access (NOMA) scheme and cognitive radio technique are utilized in IS-UAV-TN, which can improve spectrum utilization. In our paper, the transmission capacity of an NOMA-enabled IS-UAV-TN under overlay mode is discussed, specifically, we derive the closed-form expressions of ergodic capacity for both primary and secondary networks. Besides, simulation results are provided to demonstrate the validity of the mathematical derivations and indicate the influences of critical system parameters on transmission performance. Furthermore, the orthogonal multiple access (OMA)-based scheme is compared with our NOMA-based scheme as a benchmark, which illustrates that our proposed scheme has better performance.

Key words — Ergodic capacity, Integrated satellite-unmanned aerial vehicle-terrestrial networks (IS-UAV-TNs), Overlay mode, Non-orthogonal multiple access, Orthogonal multiple access, Quality-of-service.

I. Introduction

With the rapid development of wireless communication, the next generation wireless communication network must have the ability of full coverage and high rate [1]. However, owing to the low economic benefits and terrain constraints, the seamless coverage of wireless communication is far from being realized, especially in remote areas and navigation [2], [3]. Therefore, introducing satellites into the existing wireless communication network is considered to be a promising method to solve the above problem. Besides, the satellite-terrestrial network (STN) is considered to be a very significant part of the next generation wireless communication network. On the other hand, unmanned aerial vehicle (UAV) communication is an effective supplement for the satellite-terrestrial network due to its flexible operation, rapid deployment, and low-cost [4]–[6], which can eliminate the impacts of obstacles and shadow effects in the satellite-terrestrial network. At the same time, the static allocation mode of the spectrum makes the limited spectrum resources difficult to meet the growing demand. Notably, cognitive radio (CR) and non-orthogonal multiple access (NOMA) are two effective technologies that can enhance spectrum utilization respectively. Hence, this motivates us to introduce the

Manuscript Received Aug. 30, 2021; Accepted July 18, 2022. This work was supported by the National Natural Science Foundation of China (61901502, 62001517, 61971474), National Postdoctoral Program for Innovative Talents (BX20200101), and Beijing Nova Program (Z201100006820121).

 DOI:10.23919/cje.2021.00.316

cognitive radio and the non-orthogonal multiple access into our considered system to improve the transmission performance [7]–[9].

1. Related works

Nowadays, many academics and industry experts have carried out researches on STN [10]. The authors in [11] considered a land mobile satellite (LMS) with hardware impairments and interference where the satellite was utilized to be a relay to aid the communication of two terrestrial users, and the system performance was discussed. In [12], a STN with user fairness scheduling was considered, and the exact outage probability (OP) and ergodic capacity (EC) of the system were derived. Methods to improve the security and reliability of the physical layer for STN were investigated in [13], and a beamforming scheme was developed to enhance the effective achievable rate. In [14], the authors investigated the adaptive transmission schemes of STN under the condition of meeting the spectrum and power efficiency demands, and achievable channel capacity was derived. In [15], the content-based caching scheme was applied in STN, and the closed-form expression of OP was obtained. In [16], the authors investigated the performance of uplink STN with multi-relays, where the impacts of co-channel interference (CCI) as well as hardware impairments were considered.

With the unprecedented increase of UAV applications, UAV-assisted communication has been extensively employed in plenty of temporary events and natural disasters [17], [18]. The authors in [19] discussed several key enabling technologies of UAV communication over the millimeter-wave frequency band, and the challenges in this field are summarized. In [20], the authors maximized the achievable rate of millimeter-wave network based on a full-duplex UAV relay by jointly optimizing the UAV's position, beamforming, and power allocation. Two beamforming schemes based on total power and per-antenna power constraints were developed to maximize the energy efficiency (EE) of the integrated satellite-unmanned aerial vehicle-terrestrial network (IS-UAV-TN) in [17]. The authors in [21] investigated UAV-based STN with rate-splitting multiple access (RSMA), in which the sum-rate of the system was maximized. In [22], the authors optimized the EE and secure transmission of the similarity model in cognitive satellite-terrestrial networks. The authors in [5] discussed the performance of the UAV-assisted multi-relay communication network, in which the hardware impairments were considered, and the achievable sum rate was derived. In [8], the author investigated the performance of UAV-based STN with cache to reduce latency and improve file update rate. The authors in [23] studied mobile edge computing (MEC)-assisted UAV network, in which the energy consumption was optimized under allocation latency requirements and resource constraints. In [24], resources assignment of the considered UAV network was optimized with the help of the game theory, and the authors designed a multi-agent reinforcement learning framework to search for the optimal strategy. To find the resource management policy of a great quantity of UAVs, the potential game, mean-field game, Stackelberg game, graphical game, and coalition game were exploited in [25].

CR is considered as a promising way to break through the bottleneck of spectrum shortage, and the integration of CR and STN is worth exploring [26]. The authors in [26] discussed the performance of an overlay cognitive STN with secondary network selection (SNS), partial and opportunistic SNS schemes were proposed to select the proper secondary network. An EE and spectral efficiency (SE) tradeoff scheme was designed to optimize resource allocation for a cognitive satellite-vehicle network in [27]. In [28], the authors developed an adaptive transmission scheme for cognitive STN, where EE was maximized under symbol error rate (SER) constraints. The authors in [29] designed a two layer iterative beamforming scheme to take advantage of interference to improve physical layer security for cognitive STN. In [30], a beamforming scheme utilizing artificial noise and cooperative interference was adopted to improve the security of the cognitive STN in the presence of unknown eavesdroppers.

In addition, the NOMA scheme can improve the spectrum efficiency of large-scale users. The achievable rate of NOMA-based millimeter-wave communication system was maximized by optimizing power and beamforming in [31]. In [32], the authors investigated the optimization scheme of user pairing and power allocation in the NOMA network. Besides, the influences of NOMA on STN have been studied in many existing works [33], [34]. The authors in [35] investigated the NOMA-based STN with bandwidth compression (BC) to achieve non-orthogonal signals in the frequency domain and power domain, where iterative successive interference cancellation (SIC) and symmetrical coding were proposed to eliminate internal interference and reduce error probability. The authors in [36] investigated the impacts of imperfect SIC on NOMA-based STN, the exact and asymptotic OP were obtained. In [37], the influences of hardware impairments on the security of STN were investigated, and secrecy outage probability of colluding case and non-colluding case were derived. In [38] and [39], the authors investigated NOMA-based cognitive STNs, in which CR technology was applied between the primary network and secondary network, and the NOMA scheme was adopted in the process of

transmitting signals to primary users.

2. Our contributions

On the foundation, an overlay cognitive integrated satellite-UAV-terrestrial network (CIS-UAV-TN) with NOMA scheme is considered in our paper. As far as we know, no similar work has been published.

In particular, the major contributions are summed up as below:

1) First, considering the importance of STN and the flexibility of UAV, we consider a novel CIS-UAV-TN with NOMA scheme, in which the secondary network accesses the authorized spectrum of the primary network in overlay mode, and acts as a relay to assist the signal transmission of the primary network.

2) Second, probability density functions (PDFs) and cumulative distribution functions (CDFs) of shadowed-Rician (SR) fading as well as Nakagami-m fading, and Meijer-G functions are utilized to derive the closed-form expressions of EC for both the primary network and secondary network.

3) Third, simulation results are provided to demonstrate the validity of the mathematical derivations and indicate the influences of critical system parameters on transmission performance. In addition, we compare the orthogonal multiple access (OMA)-based as well as direct transmission schemes with our considered scheme to verify the superiority of our system.

II. System Model and Problem Formulation

1. System model

As shown in Fig.1 , we consider an NOMA-based CIS-UAV-TN under overlay mode, where exists a satellite-terrestrial primary network and a UAV-terrestrial-terrestrial network[*1]. In the primary network, the satellite (S) communicates with K corresponding users $\{U_i\}_{n=1}^{K}$, the NOMA scheme is applied in the transmission. Moreover, the secondary network is consist of a UAV (R) and its receiver (D). It is assumed that all nodes are equipped with a single antenna and work in half-duplex mode[*2]. Recalling the overlay mode, the secondary transmitter plays the role of the relay to forward the signal from S to U_i. As a reward, the authorized spectrum of the primary network can be utilized by the secondary network to transmit its signal. To reduce the complexity of receivers, we divide K NOMA users into 1/2 two-user groups [26], [38], thus we assume U_1 and U_2 compose a two-user group[*3]. Hence, the primary signal can be transmitted by S-U_i $(i = 1, 2)$ link and S-R-U_i link. Besides, the perfect channel state information (CSI) is assumed to be available, which can be realized by the training data and feedback from the receivers[*4] [40], [41].

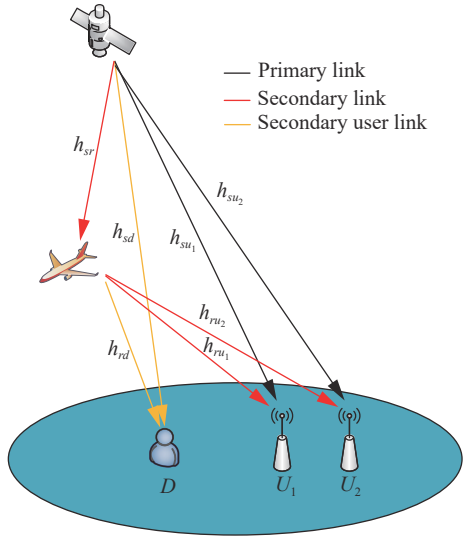

Fig. 1. System model.

The SR fading and Nakagami-m fading are utilized to model the satellite-UAV as well as satellite-terrestrial links and UAV-terrestrial links respectively[*5]. To make the expression more concise, g_{su_i}, g_{sr}, g_{sd}, h_{ru_i} and h_{rd} are defined to represent the shadowing coefficients of S-U_i link, S-R link, S-D link, R-U_i link, and R-D link respectively.

Furthermore, all receivers in our considered system suffer additive white Gaussian noise (AWGN) with $\mathcal{CN}\left(0, \sigma^2\right)$.

2. Channel model

From [42], the PDF of g_{sc} can be expressed as

$$f_{|g_{sc}|^2}(x) = \alpha_{sc} e^{-\beta_{sc} x} {}_1F_1\left(m_{sc}; 1; \delta_{sc} x\right) \tag{1}$$

where $c = \{u_i, r, d\}$, $\alpha_{sc} \triangleq \frac{1}{2b_{sc}} \left(\frac{2b_{sc} m_{sc}}{2b_{sc} m_{sc} + \Omega_{sc}}\right)^{m_{sc}}$, $\beta_{sc} \triangleq \frac{1}{2b_{sc}}$, and $\delta_{sc} \triangleq \frac{\Omega_{sc}}{2b_{sc}(2b_{sc} m_{sc} + \Omega_{sc})}$. $m_{sc} > 0$ stands for the

[*1]The scenario of CIS-UAV-TN may be represented as follows: S is a geostationary orbit (GEO) satellite, U_i denotes equipment for DVB-SH, while R and D are UAV base station and user established due to temporary activities, which is not allocated authorized spectrum.

[*2]The utilization of the single antenna is to reduce the complexity of the system, and our research can be easily extended to multi-antenna scenarios, which will be analyzed in our future work.

[*3]Two-user group scheme can reduce user interference and complexity of receivers. At the same time, this paper can be extended to multi-user scenarios, which only needs to divide multi-user into two-user pairs.

[*4]This assumption is reasonable and has been adopted in DVB-S2. Besides, our main motivation is to investigate the EC of the proposed system, and the case of imperfect CSI will be considered in our future work.

[*5]SR fading can well model satellite-UAV and satellite-terrestrial links due to its accuracy and easy calculation [17]. Moreover, Nakagami-m fading can simulate a variety of wireless fading channels by adjusting channel fading parameters m [26].

Nakagami-m parameter, $2b_{sc}$ is the average power of the multi-path part, and Ω_{sc} is the average power of line-of-sight (LOS) part.

If m_{sc} is an integer, according to the formula No.07.20.03.009.01 and formula No.07.02.03.0014.01 in [43], ${}_1F_1(m_{sc};1;\delta_{sc}x)$ can be rewritten as

$$ {}_1F_1(m_{sc};1;\delta_{sc}x)=e^{-\delta_{sc}x}\sum_{n=0}^{m_{sc}-1}\frac{(-\delta_{sc})^n(1-m_{sc})_n}{(n!)^2}x^n \tag{2}$$

In formula (2), $(.)_n$ stands for the Pochhammer symbol (see [44, p.xliii]).

By substituting (2) into (1), we can get

$$ f_{|g_{sc}|^2}(x)=\alpha_{sc}e^{-(\beta_{sc}-\delta_{sc})x}\sum_{n=0}^{m_{sc}-1}\frac{(-\delta_{sc})^n(1-m_{sc})_n}{(n!)^2}x^n \tag{3}$$

Considering the practical propagation impacts, the channel coefficients are expressed as

$$ h_{sc}=g_{sc}V_{sc} \tag{4}$$

where V_{sc} represents radio propagation loss, which consists of free space loss and radiation pattern, it can be expressed as

$$ V_{sc}=\frac{\lambda\sqrt{G_{t,sc}G_{r,sc}}}{4\pi d_{sc}\sqrt{kTB}} \tag{5}$$

where λ stands for the carrier wavelength, k represents the Boltzman constant, d_{sc} denotes the distance from the source to the destination, B is the carrier bandwidth, T denotes the noise temperature. Moreover, $G_{t,sc}$ and $G_{r,sc}$ are the antenna gain of transmitter and receiver with

$$ G_{t,sc}=G_{\max}\left(\frac{J_1(u)}{2u}+36\frac{J_3(u)}{u^3}\right)^2 \tag{6}$$

where $G_{\max}$ is the maximum of beam gain, J_n represents the n-order first-kind Bessel function, and $u=2.70123\frac{\sin\theta}{\sin\theta_{3\text{dB}}}$ with θ denotes the angle from the beam center to receiver location with regard to the S, $\theta_{3\text{dB}}$ represents the 3 dB angle.

Due to $\gamma_{sc}=\bar{\gamma}_s|h_{sc}|^2$, the PDF of γ_{sc} is given by

$$ f_{\gamma_{sc}}(x)=\alpha_{sc}\sum_{n=0}^{m_{sc}-1}\zeta(n)\,x^n e^{-\Delta_{sc}x} \tag{7}$$

where $\zeta(n)=\frac{(-\delta_{sc})^n(1-m_{sc})_n}{(n!)^2(\bar{\gamma}_s V_{sc}^2)^{n+1}}$, $\Delta_{sc}=\frac{\beta_{sc}-\delta_{sc}}{\bar{\gamma}_s}$.

With the help of formula No.3.351.2 in [44], the CDF of γ_{sc} is represented as

$$ F_{\gamma_{sc}}(x)=1-\alpha_{sc}\sum_{n=0}^{m_{sc}-1}\sum_{t=0}^{n}\frac{n!\zeta(n)}{t!\Delta_{sc}^{n-t+1}}x^t e^{-\Delta_{sc}x} \tag{8}$$

Besides, according to [26], the PDF and CDF of γ_{rj} are respectively represented by

$$ f_{\gamma_{rj}}(x)=\frac{1}{\Gamma(m_{rj})}\Xi_{rj}^{m_{rj}}x^{m_{rj}-1}e^{-\Xi_{rj}x} \tag{9}$$

and

$$ F_{\gamma_{rj}}(x)=1-e^{-\Xi_{rj}x}\sum_{p=0}^{m_{rj}-1}\frac{1}{p!}\Xi_{rj}^p x^p \tag{10}$$

where $\Xi_{rj}=\frac{m_{rj}}{\Omega_{rj}\bar{\gamma}_r}$, Ω_{rj} denotes the average power, and m_{rj} strands for the fading severity parameter.

3. Problem formulation

As shown in Fig.1 , there are two phases in the whole transmission process. In the first phase, S communicates with U_i, R, and D, where the superposition coding technique (SCT) is applied to integrate the different signals to multiple users. Hence, we can get the primary signal

$$ s_t=\sqrt{P_S\beta_1}s_1+\sqrt{P_S\beta_2}s_2 \tag{11}$$

where s_i stands for the excepted signal of U_i with $E\left(|s_i|^2\right)=1$, P_S denotes the transmit power of S, and β_i is the power assignment factor of U_i with $\beta_1+\beta_2=1$. According to the characteristics of the NOMA scheme, the transmitter assigns less power to the user with better channel quality. Without loss of genera, we assume $|h_{su_1}|^2<|h_{su_2}|^2$, thus we can get $\beta_1>\beta_2$. Besides, we can obtain the primary signals at R, D, U_i as

$$ y_{sk}=h_{sk}s_t+n_k \tag{12}$$

where $k=\{r,d,u_i\}$, n_k denotes AWGN.

In the second phase, the decode-and-forward (DF) protocol is adopted at R to transmit the expected signal of U_i. At the same time, the desired signal of D is sent by R, thus the combined signal is given by

$$ z_r=\sqrt{\mu P_R}\left(\sqrt{\beta_1}s_1+\sqrt{\beta_2}s_2\right)+\sqrt{(1-\mu)P_R}s_r \tag{13}$$

where P_R stands for the transmit power of R, s_r denotes the desired signal of D, $0<\mu<1$ is the power allocation factor.

Hence, the signals received by D and U_i is given by

$$ y_{rj}=h_{rj}z_r+n_{rj} \tag{14}$$

where $j=\{u_i,d\}$ and n_{rj} is AWGN[*6].

[*6]The received signals of two phases are combined in U_i by utilizing maximal-ratio combining (MRC).

After that, we can get the signal-to-interference plus noise ratio (SINR) of direct satellite (DS) as well as R-assisted links. To DS links, s_1 is decoded first with treating s_1 as CCI, and the SINR of s_1 at U_1 can be represented as

$$\gamma_{su_1}^{DS} = \frac{\beta_1 \gamma_{su_1}}{\beta_2 \gamma_{su_1} + 1} \tag{15}$$

where $\gamma_{su_1} = \bar{\gamma}_s |h_{su_1}|^2$ and $\bar{\gamma}_s = \frac{P_S}{\sigma^2}$.

Then, the SIC is executed at U_2 to obtain its expected signal[*7]. First, s_1 is decoded and removed from the combined signal, thus the SINR of s_1 at U_2 is given by

$$\gamma_{su_{1\to 2}}^{DS} = \frac{\beta_1 \gamma_{su_2}}{\beta_2 \gamma_{su_2} + 1} \tag{16}$$

where $\gamma_{su_2} = \bar{\gamma}_s |h_{su_2}|^2$.

Next, s_2 can be obtained only with AWGN, and the SINR of s_2 at U_2 is represented as

$$\gamma_{su_2}^{DS} = \beta_2 \gamma_{su_2} \tag{17}$$

Moreover, R and U_i perform a similar decoding process. Hence, we can obtain the SINR of s_i at R as

$$\gamma_{sr_1}^{R} = \frac{\beta_1 \gamma_{sr}}{\beta_2 \gamma_{sr} + 1} \tag{18}$$

and

$$\gamma_{sr_2}^{R} = \beta_2 \gamma_{sr} \tag{19}$$

where $\gamma_{sr} = \bar{\gamma}_s |h_{sr}|^2$.

In addition, the SINR of s_i at U_i are given by

$$\gamma_{ru_1}^{R} = \frac{\beta_1 \mu \gamma_{ru_1}}{\tau_1 \gamma_{ru_1} + 1} \tag{20}$$

$$\gamma_{ru_{1\to 2}}^{R} = \frac{\beta_1 \mu \gamma_{ru_2}}{\tau_1 \gamma_{ru_2} + 1} \tag{21}$$

and

$$\gamma_{ru_2}^{R} = \frac{\beta_2 \mu \gamma_{ru_2}}{\tau_2 \gamma_{ru_2} + 1} \tag{22}$$

where $\tau_1 = \beta_2 \mu + 1 - \mu$, $\tau_2 = 1 - \mu$, $\gamma_{ru_1} = \bar{\gamma}_r |h_{ru_1}|^2$, $\gamma_{ru_2} = \bar{\gamma}_r |h_{ru_2}|^2$, $\bar{\gamma}_r = \frac{P_R}{\sigma^2}$.

By the same way, the SINR at D can be expressed as

$$\gamma_{rd}^{R} = \frac{(1-\mu)\gamma_{rd}}{\mu \gamma_{rd} + 1} \tag{23}$$

where $\gamma_{rd} = \bar{\gamma}_r |h_{rd}|^2$.

III. EC of the CIS-UAV-TN

EC is a significant indicator to measure the performance of the wireless system. It represents the time average of the maximum information rate in all fading states between the transmitter and receiver. In this section, we derive the exact expressions of EC for both the primary network and secondary network.

1. EC of the primary network

In general, we define the EC of R-assisted link as the minimal EC of the two phases [45]. Therefore, we can represent the EC of the primary network as

$$EC_{total} = EC_{DS} + EC_R \tag{24}$$

where EC_{DS} denotes EC of the DS links, and $EC_R = \min(EC_{SR}, EC_{RU})$ stands for EC of the R-assisted link with EC_{SR} being EC of S-R link and EC_{RU} being that of R-U_i link.

First, we derive the expression of EC_{DS}. According to the definition of EC, EC_{DS} is given by

$$\begin{aligned} EC_{DS} =& E\left[\log_2\left(1+\gamma_{su_1}^{DS}\right)\right] + E\left[\log_2\left(1+\gamma_{su_{1\to 2}}^{DS}\right)\right] \\ &+ E\left[\log_2\left(1+\gamma_{su_2}^{DS}\right)\right] \end{aligned} \tag{25}$$

By taking (15), (16), and (17) into (25), we can get

$$\begin{aligned} EC_{DS} =& \frac{1}{\ln 2}\left\{E\left[\ln\left(1+\gamma_{su_1}\right)\right] + E\left[\ln\left(1+\gamma_{su_2}\right)\right]\right. \\ &\left. - E\left[\ln\left(1+\beta_2\gamma_{su_1}\right)\right]\right\} \end{aligned} \tag{26}$$

Let $\beta_2 \gamma_{su_1} = z$, by utilizing the probability transformation formula $\left(t = Ax \to f_t(t) = \frac{1}{A} f_x\left(\frac{x}{A}\right)\right)$, the PDF of z can be obtained as

$$f_z(z) = \alpha_{su_1} \sum_{n=0}^{m_{su_1}-1} \left(\frac{1}{\beta_2}\right)^{n+1} \zeta(n)\, z^n e^{-\frac{\Delta_{su_1}}{\beta_2} z} \tag{27}$$

Then, formula (26) is re-written as

$$\begin{aligned} EC_{DS} =& \frac{1}{\ln 2}\left\{\int_0^\infty \ln(1+x) f_{\gamma_{su_1}}(x)\, dx \right. \\ &+ \int_0^\infty \ln(1+y) f_{\gamma_{su_2}}(y)\, dy \\ &\left. - \int_0^\infty \ln(1+z) f_z(z)\, dz \right\} \end{aligned} \tag{28}$$

By substituting $\ln(1+x) = G_{2,2}^{1,2}\left[x \middle| \begin{matrix} 1,1 \\ 1,0 \end{matrix}\right]$, (7), and (27) into (28), we can get (29) as following, where $G_{p,q}^{m,n}\left(x \middle| \begin{matrix} a_1, & \ldots, & a_p \\ b_1 & \ldots, & b_q \end{matrix}\right)$ is Meijer-G function (see for-

[*7]Imperfect SIC is beyond the research scope of this paper. We will consider it in our follow-up research.

mula No.9.301 in [33]).

$$EC_{DS} = \frac{1}{\ln 2}\left\{\int_0^{\infty} G_{2,2}^{1,2}\left[x\middle|\begin{matrix}1,1\\1,0\end{matrix}\right]\alpha_{su_1}\sum_{n=0}^{m_{su_1}-1}\zeta(n)x^n e^{-\Delta_{su_1}x}dx + \int_0^{\infty} G_{2,2}^{1,2}\left[y\middle|\begin{matrix}1,1\\1,0\end{matrix}\right]\alpha_{su_2}\sum_{n=0}^{m_{su_2}-1}\zeta(n)y^n e^{-\Delta_{su_2}y}dy - \int_0^{\infty} G_{2,2}^{1,2}\left[z\middle|\begin{matrix}1,1\\1,0\end{matrix}\right]\alpha_{su_1}\sum_{n=0}^{m_{su_1}-1}\left(\frac{1}{\beta_2}\right)^{n+1}\zeta(n)z^n e^{-\frac{\Delta_{su_1}}{\beta_2}z}dz\right\} \tag{29}$$

With the help of the formula No.2.24.3.1 in [46], the exact expression of EC_{DS} can be obtained as (30).

$$EC_{DS} = \frac{1}{\ln 2}\left\{\alpha_{su_1}\sum_{n=0}^{m_{su_1}-1}\zeta(n)\Delta_{su_1}^{-(n+1)}\left[G_{3,2}^{1,3}\left[\frac{1}{\Delta_{su_1}}\middle|\begin{matrix}-n,1,1\\1,0\end{matrix}\right] - G_{3,2}^{1,3}\left[\frac{\beta_2}{\Delta_{su_1}}\middle|\begin{matrix}-n,1,1\\1,0\end{matrix}\right]\right] + \alpha_{su_2}\sum_{n=0}^{m_{su_2}-1}\zeta(n)\Delta_{su_2}^{-(n+1)}G_{3,2}^{1,3}\left[\frac{1}{\Delta_{su_z}}\middle|\begin{matrix}-n,1,1\\1,0\end{matrix}\right]\right\} \tag{30}$$

To solve the situation that $\Delta_{su_i}=0$, by applying the formula No.8.2.2.14 in [46]:

$$G_{p,q}^{m,n}\left[t\middle|\begin{matrix}(a_p)\\(b_q)\end{matrix}\right] = G_{q,p}^{n,m}\left[\frac{1}{t}\middle|\begin{matrix}1-(b_q)\\1-(a_p)\end{matrix}\right] \tag{31}$$

EC_{DS} can be re-written as (32).

$$EC_{DS} = \frac{1}{\ln 2}\left\{\alpha_{su_1}\sum_{n=0}^{m_{su_1}-1}\zeta(n)\Delta_{su_1}^{-(n+1)}\left[G_{2,3}^{3,1}\left[\Delta_{su_1}\middle|\begin{matrix}0,1\\1+n,1,1\end{matrix}\right] - G_{2,3}^{3,1}\left[\frac{\Delta_{su_1}}{\beta_2}\middle|\begin{matrix}0,1\\1+n,1,1\end{matrix}\right]\right] + \alpha_{su_2}\sum_{n=0}^{m_{su_2}-1}\zeta(n)\Delta_{su_2}^{-(n+1)}G_{2,3}^{3,1}\left[\Delta_{su_2}\middle|\begin{matrix}0,1\\1+n,1,1\end{matrix}\right]\right\} \tag{32}$$

By the similar derivation, EC_{SR} and EC_{RU} can be obtained as (33) and (34), respectively.

$$EC_{SR} = \frac{1}{2}\left\{E\left[\log_2\left(1+\gamma_{sr_1}^R\right)\right] + E\left[\log_2\left(1+\gamma_{sr_2}^R\right)\right]\right\} = \frac{1}{2\ln 2}\alpha_{sr}\sum_{n=0}^{m_{sr}-1}\zeta(n)\Delta_{sr}^{-(n+1)}G_{2,3}^{3,1}\left[\Delta_{sr}\middle|\begin{matrix}0,1\\1+n,1,1\end{matrix}\right] \tag{33}$$

$$EC_{RU} = \frac{1}{2}\left\{E\left[\log_2\left(1+\gamma_{ru_1}^R\right)\right] + E\left[\log_2\left(1+\gamma_{ru_{1\to 2}}^R\right)\right] + E\left[\log_2\left(1+\gamma_{ru_2}^R\right)\right]\right\} = \frac{1}{2\ln 2}\left\{\frac{1}{\Gamma(m_{ru_1})}\left[G_{2,3}^{3,1}\left[\Xi_{ru_1}\middle|\begin{matrix}0,1\\1+n,1,1\end{matrix}\right] - G_{2,3}^{3,1}\left[\frac{\Xi_{ru_1}}{\tau_1}\middle|\begin{matrix}0,1\\1+n,1,1\end{matrix}\right]\right] + \frac{1}{\Gamma(m_{ru_2})}\left[G_{2,3}^{3,1}\left[\Xi_{ru_2}\middle|\begin{matrix}0,1\\1+n,1,1\end{matrix}\right] - G_{2,3}^{3,1}\left[\frac{\Xi_{ru_2}}{\tau_2}\middle|\begin{matrix}0,1\\1+n,1,1\end{matrix}\right]\right]\right\} \tag{34}$$

Noting that 1/2 is necessary because of DF protocol.

2. EC of the secondary network

The EC of the secondary network is expressed as

$$EC_{SN} = \frac{1}{2}E\left[\log_2\left(1+\gamma_{rd}\right)\right] \tag{35}$$

With the similar method of obtaining the EC of the primary network, we can get the exact EC_{SN} as

$$EC_{SN} = \frac{1}{2\ln 2}\frac{1}{\Gamma(m_{rd})}\times\left[G_{2,3}^{3,1}\left[\Xi_{rd}\middle|\begin{matrix}0,1\\m_{rd},1,1\end{matrix}\right] - G_{2,3}^{3,1}\left[\frac{\Xi_{rd}}{\mu}\middle|\begin{matrix}0,1\\m_{rd},1,1\end{matrix}\right]\right] \tag{36}$$

IV. Numerical Results

In this section, simulations are conducted to demonstrate the validity of our derivation. The simulation tool is MATLAB 2019. In general, we set $\overline{\gamma}_s = \overline{\gamma}_r = \overline{\gamma}$, and other system parameters and channel parameters are shown in Table 1 and Table 2 [38], [31].

First, we can clearly see that the theoretical analysis coincides with Monte Carlo (MC) simulations, which testifies the correctness of our analysis. Besides, our considered system has higher EC than only the DS system. It proves our considered system has better transmission capability.

Fig.2 shows the EC of primary network with different $\overline{\gamma}$, we set $m_{rj}=2$, $\beta_1=0.67$, $\mu=0.92$. It is clear that the EC of the primary network increase with $\overline{\gamma}$. This is because the enhancement of SNR can improve transmission performance.

Table 1. System parameters

Parameter name	Parameter value
Satellite	GEO
f	2 GHz
$\theta_{3\text{dB}}$	0.8°
$G_{\max}$	48 dB
$G_{r,p}$	4 dB
B	15 MHz
k	1.38×10^{-23} J/K
T	300°
σ^2	1
Ω_{rj}	1

Table 2. Channel parameters

Shadowing	m	b	Ω
Infrequent light shadowing (ILS)	10	0.158	1.29
Average shadowing (AS)	5	0.251	0.279
Frequent heavy shadowing (FHS)	1	0.063	0.0007

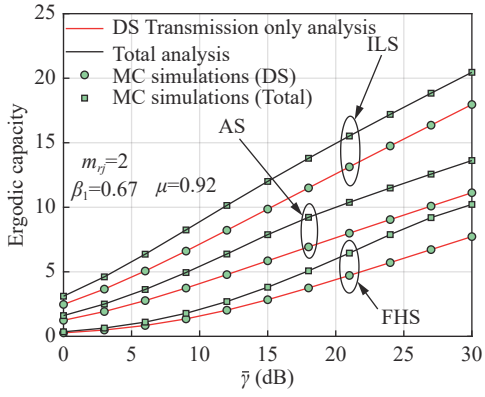

Fig. 2. The EC of primary network with different $\overline{\gamma}$.

Fig.3 illustrates the EC of primary network with different μ with setting $m_{rj}=2$, $\beta_1=0.67$, $\overline{\gamma}=30$ dB.

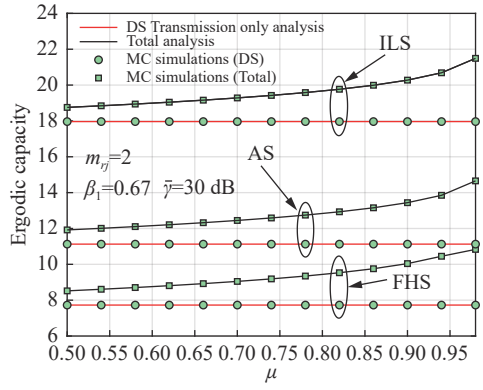

Fig. 3. The EC of primary network with different μ.

It can be found that our proposed system has better performance with the increase of μ, it is due to the fact that the raise of μ indicates that R assigns more power to transmit the signal of the primary network, which will lead to the enhancement of the SNR. Furthermore, the EC of only the DS transmission scheme is uncorrelated with μ. It can be explained by the reason that the transmission in the first phase may not be affected by μ. Besides, our proposed system has better performance under ILS and worse performance under FHS.

Fig.4 plots the EC of primary network with different β_1 with $m_{rj}=2$, $\mu=0.92$, $\overline{\gamma}=30$ dB. Transmission performance of both our considered scheme and only DS transmission scheme perform better with large β_1, which shows that assigning more power to users with worse channel quality leads to the improvement of EC. Notably, this phenomenon is different from the properties of OP for the NOMA system, which has an optimal power allocation factor less than 1. It is due to the fact that large β_1 will lead to the outage of U_2.

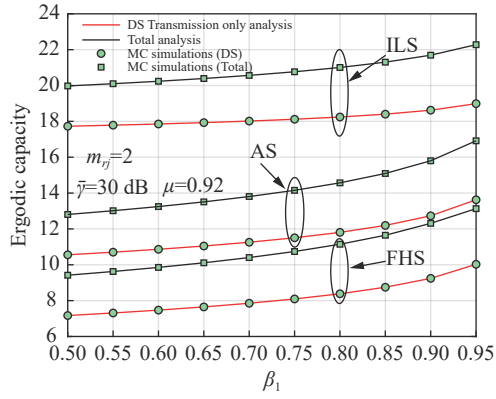

Fig. 4. The EC of primary network with different β_1.

Fig.5 depicts the EC of primary network with NOMA and OMA, we set $m_{rj}=2$, $\beta_1=0.67$, $\mu=0.92$. We can easily find that the OMA-based system performs worse than our considered NOMA-based system.

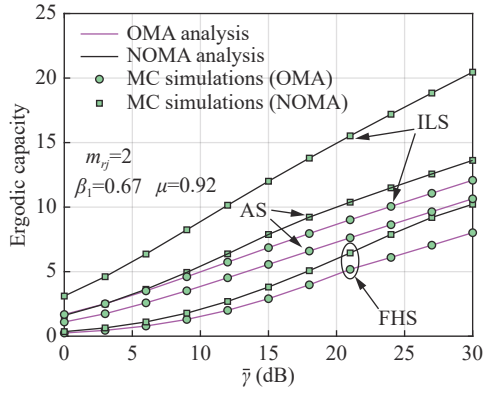

Fig. 5. The EC of primary network with different NOMA and OMA.

Besides, with the improvement of average SNR, the gaps of curves with different channel conditions become larger, or our proposed system has more obvious advantages than the traditional OMA system.

Fig.6 depicts the EC of secondary network with different $\overline{\gamma}$ with $\beta_1 = 0.67$ and FHS. The transmission performance of secondary network enhances with $\overline{\gamma}$. Besides, the larger m_{rj} means the better channel quality, which leads to the enhancement of system performance. Contrary to the primary network, diminishing μ will improve the EC of the secondary network. Hence, R can balance the performance of the primary network and secondary network by adjusting μ.

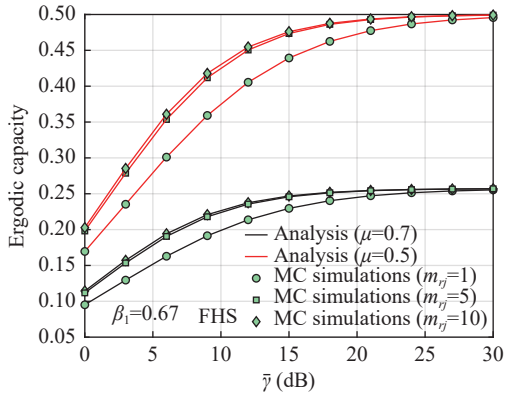

Fig. 6. The EC of secondary network with different $\overline{\gamma}$.

V. Conclusions

In our paper, an NOMA-based CIS-UAV-TN work in overlay mode was studied, in which the primary signal was forwarded by the secondary transmitter to enhance the EC of the primary network, and the secondary network obtained the opportunity to access its spectrum. Specifically, with the utilization of the statistical expressions of SR fading and Nakagami-m fading, the exact EC of both the two networks were derived. Simulation results were provided, which indicated that the transmission performance of our considered system can be enhanced by adjusting the power allocation factor and power assignment factor.

References

[1] M. Jia, X. Gu, Q. Guo, *et al.*, "Broadband hybrid satellite-terrestrial communication systems based on cognitive radio toward 5G," *IEEE Wireless Commun.* , vol.23, no.6, pp.96–106, 2016.

[2] K. Guo, K. An, B. Zhang, *et al.*, "Physical layer security for multiuser satellite communication systems with threshold-based scheduling scheme," *IEEE Trans. Vehi. Tech.*, vol.69, no.5, pp.5129–5141, 2020.

[3] M. Jia, X. Zhang, J. Sun, *et al.*, "Intelligent resource management for satellite and terrestrial spectrum shared networking toward B5G," *IEEE Wireless Commun.* , vol.27, no.1, pp.54–61, 2020.

[4] C. Dong, Y. Shen, Y. Qu, *et al.*, "UAVs as an intelligent service: boosting edge intelligence for air-ground integrated networks," *IEEE Netw.*, vol.35, no.4, pp.167–175, 2021.

[5] X. Li, Q. Wang, Y. Liu, *et al.*, "UAV-aided multi-way NOMA networks with residual hardware impairments," *IEEE Wireless Communi. Lett.*, vol.9, no.9, pp.1538–1542, 2020.

[6] J. Chen, Q. Wu, Y. Xu, *et al.*, "Spectrum allocation for task-driven UAV communication networks exploiting game theory," *IEEE Trans. Commun.* , vol.28, no.4, pp.174–181, 2021.

[7] Q. Wu, G. Ding, Y. Xu, *et al.*, "Cognitive internet of things: A new paradigm beyond connection," *IEEE Internet Things J.*, vol.1, no.2, pp.129–143, 2014.

[8] X. Zhang, B. Zhang, K. An, *et al.*, "Stochastic geometry-based analysis of cache-enabled hybrid satellite-aerial-terrestrial networks with non-orthogonal multiple access," *IEEE Trans. Wireless Communi.*, vol.21, no.2, pp.1272–1287, 2022.

[9] Z. Lin, M. Lin, W. -P. Zhu, *et al.*, "Robust secure beamforming for wireless powered cognitive satellite-terrestrial networks," *IEEE Trans. Cogn. Commun.* , vol.7, no.2, pp.567–580, 2021.

[10] X. Zhang, D. Guo, K. An, *et al.*, "Auction-based multichannel cooperative spectrum sharing in hybrid satellite-terrestrial IoT networks," *IEEE Internet Things J.*, vol.8, no.8, pp.7009–7023, 2021.

[11] K. Guo, M. Lin, B. Zhang, *et al.*, "On the performance of LMS communication with hardware impairments and interference," *IEEE Trans. Commun.* , vol.67, no.2, pp.1490–1505, 2019.

[12] Q. Huang, M. Lin, W. -P. Zhu, *et al.*, "Performance analysis of integrated satellite-terrestrial multiantenna relay networks with multiuser scheduling," *IEEE Trans. Aerosp. Electron. Syst.*, vol.56, no.4, pp.2718–2731, 2020.

[13] M. Lin, Q. Huang, T. de Cola, *et al.*, "Integrated 5G-satellite networks: A perspective on physical layer reliability and security," *IEEE Wireless Commun.* , vol.27, no.6, pp.152–159, 2020.

[14] K. An and T. Liang, "Hybrid satellite-terrestrial relay networks with adaptive transmission," *IEEE Trans. Vehi. Tech.*, vol.68, no.12, pp.12448–12452, 2019.

[15] K. An, Y. Li, X. Yan, and T. Liang, "On the performance of cache-enabled hybrid satellite-terrestrial relay networks," *IEEE Wireless Commun. Lett.*, vol.8, no.5, pp.1506–1509, 2019.

[16] K. Guo, K. An, B. Zhang, Y. Huang, *et al.*, "On the performance of the uplink satellite multi-terrestrial relay networks with hardware impairments and interference," *IEEE Syst. J.*, vol.13, no.3, pp.2297–2308, 2019.

[17] Q. Huang, M. Lin, J. Wang, T. A. Tsiftsis, *et al.*, "Energy efficient beamforming schemes for satellite-aerial-terrestrial networks," *IEEE Trans. Commun.* , vol.68, no.6, pp.3863–3875, 2020.

[18] X. Liu, Y. Liu, and Y. Chen, "Machine learning empowered trajectory and passive beamforming design in UAV-RIS wireless networks," *IEEE J. Sel. Areas Commun.*, vol.39, no.7, article no.2055, 2021.

[19] Z. Xiao, L. Zhu, and X. -G. Xia, "UAV communications with millimeter-wave beamforming: Potentials, scenarios,

and challenges," *China Communi.*, vol.17, no.9, pp.147–166, 2020.

[20] L. Zhu, J. Zhang, Z. Xiao, *et al.*, "Millimeter-wave full-duplex UAV relay: Joint positioning, beamforming, and power control," *IEEE J. Sel. Areas Commun.* , vol.38, no.9, pp.2057–2073, 2020.

[21] Z. Lin, M. Lin, T. de Cola, J. -B. Wang, *et al.*, "Supporting IoT with rate-splitting multiple access in satellite and aerial-integrated networks," *IEEE Internet Things J.*, vol.8, no.14, pp.11123–11134, 2021.

[22] Z. Lin, M. Lin, B. Champagne, *et al.*, "Secure and energy efficient transmission for RSMA-based cognitive satellite-terrestrial networks," *IEEE Wireless Communi. Lett.*, vol.10, no.2, pp.251–255, 2021.

[23] Y. Qu, H. Dai, H. Wang, *et al.*, "Service provisioning for UAV-enabled mobile edge computing," *IEEE J. Sel. Areas Commun.*, vol.39, no.11, pp.3287–3305, 2021.

[24] J. Cui, Y. Liu, and A. Nallanathan, "Multi-agent reinforcement learning-based resource allocation for UAV networks," *IEEE Trans. Wireless Commun.*, vol.19, no.2, pp.729–743, 2020.

[25] J. Chen, P. Chen, Q. Wu, *et al.*, " A game-theoretic perspective on resource management for large-scale UAV communication networks," *China Commun.* , vol.18, no.1, pp.70–87, 2021.

[26] P. K. Sharma, P. K. Upadhyay, D. B. da Costa, *et al.*, "Performance analysis of overlay spectrum sharing in hybrid satellite-terrestrial systems with secondary network selection," *IEEE Trans. Wireless Commun.* , vol.16, no.10, pp.6586–6601, 2017.

[27] Y. Ruan, Y. Li, C. Wang, R. Zhang, *et al.*, "Power allocation in cognitive satellite-vehicular networks from energy-spectral efficiency tradeoff perspective," *IEEE Trans. Cogn. Commun.*, vol.5, no.2, pp.318–329, 2019.

[28] Y. Ruan, Y. Li, C. Wang, and R. Zhang, "Energy efficient adaptive transmissions in integrated satellite-terrestrial networks with SER constraints," *IEEE Trans. Wireless Commun.*, vol.17, no.1, pp.210–222, 2018.

[29] M. Lin, Z. Lin, W. Zhu, and J. Wang, "Joint beamforming for secure communication in cognitive satellite terrestrial networks," *IEEE J. Sel. Areas Commun.* , vol.36, no.5, pp.1017–1029, 2018.

[30] Z. Lin, M. Lin, B. Champagne, *et al.*, "Secure beamforming for cognitive satellite terrestrial networks with unknown eavesdroppers," *IEEE Syst. J.* , vol.15, no.2, pp.2186–2189, 2021.

[31] L. Zhu, J. Zhang, Z. Xiao, X. Cao, *et al.*, "Millimeter-wave NOMA with user grouping, power allocation and hybrid beamforming," *IEEE Trans. Wireless Communi.* , vol.18, no.11, pp.5065–5079, 2019.

[32] L. Zhu, J. Zhang, Z. Xiao, X. Cao, and D. O. Wu, "Optimal user pairing for downlink non-orthogonal multiple access (NOMA)," *IEEE Wireless Commun. lett.* , vol.8, no.2, pp.328–331, 2019.

[33] X. Zhang, K. An, B. Zhang, *et al.*, "Vickrey auction-based secondary relay selection in cognitive hybrid satellite-terrestrial overlay networks with non-orthogonal multiple access," *IEEE Wireless. Commun. Lett.* , vol.9, no.5, pp.628–632, 2020.

[34] X. Zhang, B. Zhang, K. An, *et al.*, "Outage performance of NOMA-based cognitive hybrid satellite-terrestrial overlay networks by amplify-and-forward protocols," *IEEE Access*, vol.7, pp.85372–85381, 2019.

[35] M. Jia, Q. Gao, Q. Guo, X. Gu, and X. Shen, "Power multiplexing NOMA and bandwidth compression for satellite-terrestrial networks," *IEEE Trans. Vehi. Tech.*, vol.68, no.11, pp.11107–11117, 2019.

[36] X. Yue, Y. Liu, Y. Yao, T. Li, *et al.*, "Outage behaviors of NOMA-based satellite network over shadowed-rician fading channels," *IEEE Trans. Vehi. Tech.*, vol.69, no.6, pp.6818–6821, 2020.

[37] K. Guo, K. An, F. Zhou, T. Tsiftsis, *et al.*, "On the secrecy performance of NOMA-based integrated satellite multiple-terrestrial relay networks with hardware impairments," *IEEE Trans. Vehi. Tech.*, vol.70, no.4, pp.3661–3676, 2021.

[38] R. Liu, K. Guo, K. An, S. Zhu, *et al.*, "NOMA-based integrated satellite-terrestrial relay networks under spectrum sharing environment," *IEEE Wireless Commun. Lett.*, vol.10, no.6, pp.1266–1270, 2021.

[39] R. Liu, K. Guo, K. An, S. Zhu, *et al.*, "Performance evaluation of NOMA-based cognitive integrated satellite terrestrial relay networks with primary interference," *IEEE Access*, vol.9, pp.71422–71434, 2021.

[40] M. K. Arti, "Channel estimation and detection in satellite communication systems," *IEEE Trans. Vehi. Tech.*, vol.65, no.12, pp.10173–10179, 2016.

[41] M. R. Bhatnagar, "Making two-way satellite relaying feasible: A differential modulation based approach," *IEEE Trans. Commun.*, vol.63, no.8, pp.2836–2847, 2015.

[42] N. I. Miridakis, D. D. Vergados, and A. Michalas, "Dual-hop communication over a satellite relay and Shadowed Rician channels," *IEEE Trans. Vehi. Tech.* , vol.64, no.9, pp.4031–4040, 2015.

[43] Wolfram Research, Inc., "The mathematical functions site," Available at: *http://functions.wolfram.com*, 2021.

[44] I. S. Gradshteyn, I. M. Ryzhik, A. Jeffrey, *et al.*, *Table of Integrals, Series and Products*, 7th ed., Amsterdam, Elsevier, Boston, Massachusetts, USA, 2007.

[45] G. Farhadi and N. C. Beaulieu, "On the ergodic capacity of multi-hop wireless relaying systems," *IEEE Trans. Wireless Commun.*, vol.8, no.8, pp.2286–2291, 2009.

[46] A. P. Prudnikov, Y. A. Brychkov, and O. I. Marichev, *Integrals and Series, Volume 3: More Special Functions*, Gordon and Breach Science Publishers, New York, USA, 1990.

GUO Kefeng received the B.S. degree from Beijing Institute of Technology, Beijing, China, in 2012, the M.S. degree from PLA University of Science and Technology, Nanjing, China, in 2015, and the Ph.D. degree in Army Engineering University of PLA in 2018. He is an Associate Professor in the College of Electronic and Information Engineering, Nanjing University of Aeronautics and Astronautics. His research interests focus on cooperative relay networks, MIMO communications systems, multiuser communication systems, satellite communication, hardware impairments, cognitive radio and physical layer security. Dr. Guo has been the TPC Member of many IEEE sponsored conferences, such as IEEE ICC, IEEE GLOBECOM and IEEE WCNC. (Email: guokefeng.cool@163.com)

LIU Rui received the B.S. degree from Space Engineering University, Beijing, China, in 2019. He is currently working toward the Ph.D. degree in Space Engineering University. His research interests focus on satellite-terrestrial networks, cognitive radio systems, wireless communication systems, and multiuser communication system.
(Email: lrevri@163.com)

DONG Chao received the Ph.D. degree in communication engineering from PLA University of Science and Technology, China, in 2007. He is now a Full Professor with the College of Electronic and Information Engineering, Nanjing University of Aeronautics and Astronautics, China. His current research interests include D2D, UAV networking, and anti-jamming. (Email: dch@nuaa.edu.cn)

AN Kang received the B.S. degree from Nanjing University of Aeronautics and Astronautics, Nanjing, China, in 2011, the M.S. degree from the PLA University of Science and Technology, Nanjing, China, and the Ph.D. degree in Army Engineering University of PLA in 2017. He is currently an Engineer in the Sixty-third Research Institute, National University of Defense Technology, Nanjing. His research interests include cooperative communication, satellite communication, cognitive radio and physical layer security.
(Email: ankang89@nudt.edu.cn)

HUANG Yuzhen received the B.S. degree in communications engineering and the Ph.D. degree in communications and information systems from the College of Communications Engineering, PLA University of Science and Technology, Nanjing, China, in 2008 and 2013, respectively. Since 2018, he has been with the Artificial Intelligence Research Center, National Innovation Institute of Defense Technology, Beijing, China, where he is currently an Associate Professor. He is also a Postdoctoral Research Associate with the School of Information and Communication, Beijing University of Posts and Telecommunications, Beijing. He has authored or coauthored nearly 90 research papers in international journals and conferences. His research interests include channel coding, MIMO communications systems, cooperative communications, physical layer security, and cognitive radio systems. He and his coauthors were awarded a Best Paper Award at the WCSP 2013. He was the recipient of an IEEE Communications Letters Exemplary Reviewer Certificate for 2014. He is an Associate Editor for the KSII Transactions on Internet and Information Systems. (Email: yzh_huang@sina.com)

ZHU Shibing received the B.S. degree from Equipment College, Beijing, China, in 1992, the M.S. degree from National Defense University, Beijing, China, in 1997, and the Ph.D. degree from the Wuhan University of Technology, Wuhan China, in 2009. He is currently a Professor and a Doctoral Supervisor in Space Engineering University. His current research interests include spatial information network and security, and 5G mobile communication.
(Email: sbz_zhu@sohu.com)